13A.3 Simulating Supercell Thunderstorms in a Horizontally-Heterogeneous Convective Boundary Layer

CHRISTOPHER J. NOWOTARSKI,* PAUL M. MARKOWSKI, AND YVETTE P. RICHARDSON

Department of Meteorology, The Pennsylvania State University, University Park, PA

GEORGE H. BRYAN

National Center for Atmospheric Research, Boulder, CO

1. Introduction

Despite the heterogeneous nature of the atmosphere, an overwhelming majority of studies incorporating numerical simulations of supercell thunderstorms have used a horizontally-homogeneous base state. Numerical simulations and observations alike have shown the importance of vertical wind shear and buoyancy in determining the mode and behavior of deep moist convection. Storms can be especially sensitive to the vertical profiles of temperature, moisture, and wind in the lowest 1000 m (e.g., supercells are more likely to be tornadic when the boundary layer is characterized by high relative humidity and vertical shear relative to the average environment supportive of supercells; Markowski and Richardson 2009). Given these sensitivities, we expect that horizontal variations in temperature, moisture, and wind, particularly in the boundary layer, will affect the behavior of simulated supercell thunderstorms.

Several previous studies have examined the effects of mesoscale variability on both simulated and observed storms. Richardson et al. (2007) found that horizontal variations in background vertical wind shear of meso-β scale "profoundly influence the morphology of deep convective storms." In their simulations, storm propagation via the development of new cells was related to variations of shear across the system. Storms were found to transition into stronger, more organized modes when the initial cells moved into areas of greater vertical wind shear. Richardson (1999) found that multicell systems tend to propagate toward areas of increased low-level moisture in weak shear regimes because new cell development was more favorable in such locations. Furthermore, isolated supercells in areas of increased low-level moisture exhibited both higher updraft speed and stronger low-level rotation.

Investigations including environmental variability on the meso-γ scale have been limited (see Peckham et al. 2004; Carpenter et al. 1998; Knopfmeier et al. 2008). Convective boundary layers (CBLs) are characterized by such heterogeneity, and one would expect a CBL to be present in most daytime severe storm environments. Thermals in a CBL can be organized into coherent patterns (e.g., cells, rolls) depending on the magnitude of the vertical wind shear, surface buoyancy flux, and boundary layer depth. The details of a given day are usually sufficiently complicated so as to make it difficult to precisely anticipate the structure of BL convection (e.g., there can be thermal as well as dynamical instabilities realized, as well as interactions between convection and gravity waves triggered by the penetration of a capping inversion by the convection). However, there is a rough tendency for cells to occur in conditions of light winds (and therefore weak near-surface shear), strong buoyancy flux, and a deep boundary layer, and rolls (hereafter horizontal convective rolls, or HCRs) to occur in conditions of strong winds (and therefore strong near-surface shear), weak buoyancy flux, and a shallow boundary layer (Weckwerth et al. 1999). A transition from rolls to cells (in light winds) or disorganized convection (in strong winds) often occurs as the buoyancy flux increases and the boundary layer deepens during the day. Because supercells, especially those that become tornadic, require sufficient low-level vertical wind shear, the ambient CBL is most likely characterized by HCRs rather than cells. Depending on the convective and dynamic instabilities present in the environment, HCR wavelengths may vary from 2-20 km with vertical velocity perturbations generally less than 5 m s^{-1} (Etling and Brown 1993).

HCRs lead to horizontal heterogeneity in the low-level thermodynamic and kinematic fields due to periodic variations in vertical velocity (and by extension, convergence) associated with them. Weckwerth et al. (1996) found a difference in potential temperature of 0.5 K between the updraft and downdraft branches of HCRs and water vapor mixing ratio difference of 1.5-2.5 g kg^{-1}. This moisture variability results from updraft branches converging and lifting surface moisture into the CBL while downdraft branches force drier air from aloft towards the ground. Consequently, CAPE is generally higher within HCR updraft branches and lifting condensation levels are lower. Markowski and Richardson (2007) found horizontal variations in low-level wind shear within observed CBLs wherein 0-1 km wind shear was found to vary as much as 5 m s^{-1} within the same mesoscale airmass. Additionally, local maxima in vertical wind shear caused by boundary layer convection were found to be located where the magnitude of CBL vertical velocity was a minimum. Thus, it seems that maxima in buoyancy and shear perturbations resulting from boundary layer convection are not co-located.

Because boundary layer convection is driven in part by the convective instability that results from daytime surface heating, it is likely that any storm-induced variations in surface temperature may affect the evolution of the CBL. Markowski et al. (1998) showed that near-surface temperature can decrease by

**Corresponding author address*: Christopher Nowotarski, Department of Meteorology, Pennsylvania State University, 503 Walker Building, University Park, PA 16802; *e-mail*: cjn5012@psu.edu.

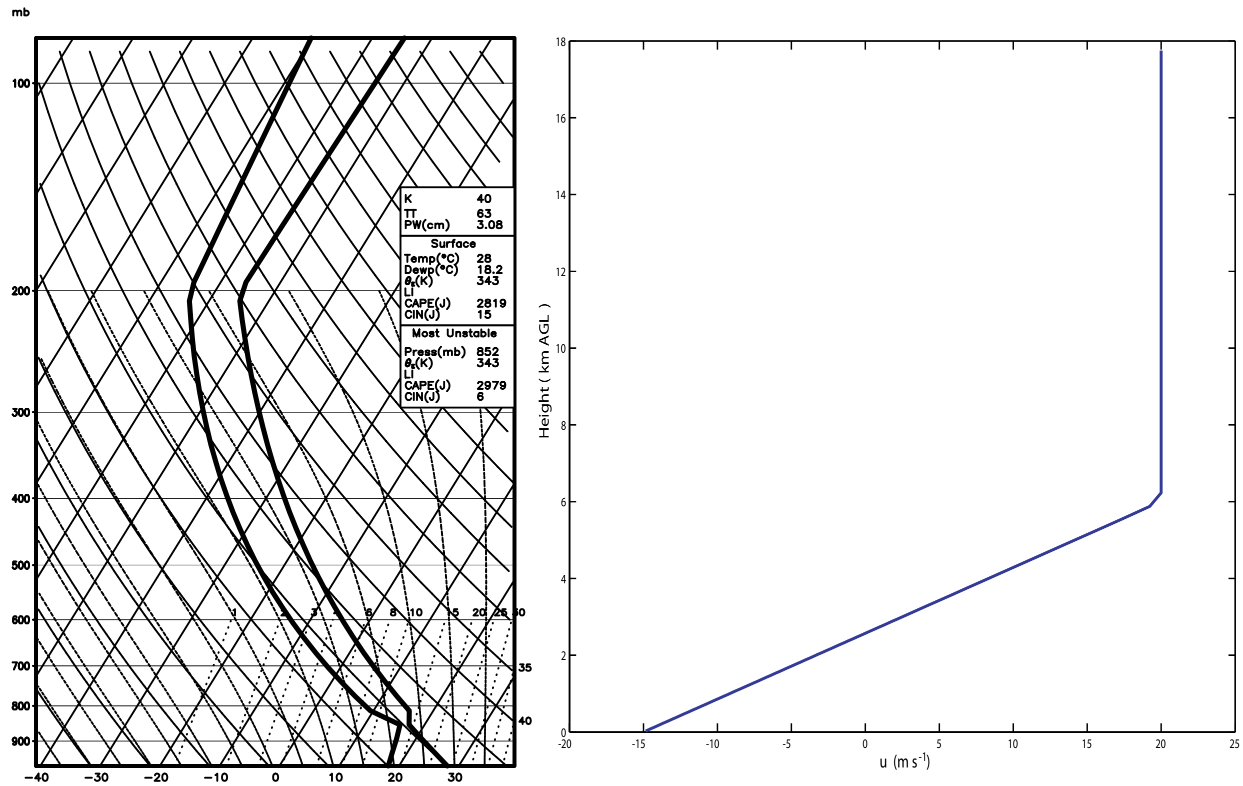

FIG. 1. The initial thermodynamic and unidirectional wind profiles used in the CBL simulation. Random potential temperature perturbations are added in the boundary layer before the model is initialized.

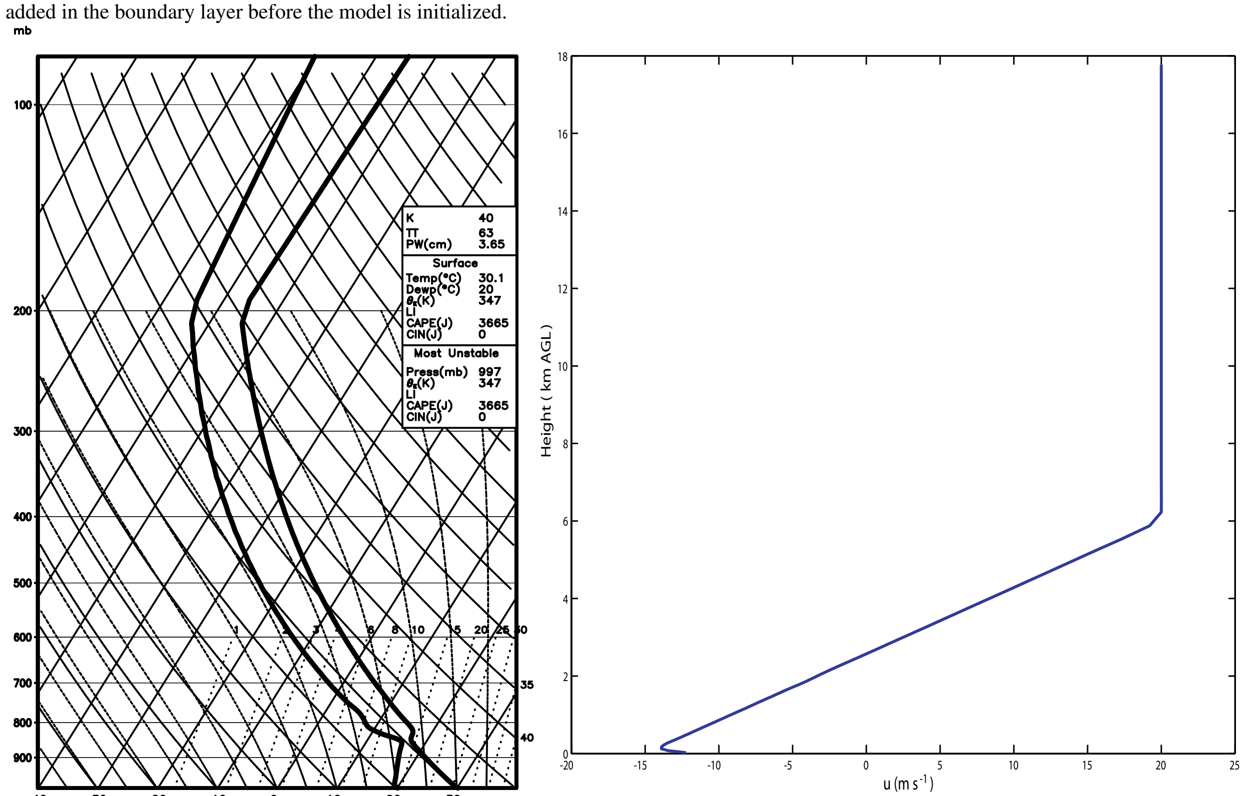

FIG. 2. The domain-averaged thermodynamic and u wind component profile after one hour in the CBL simulation. These profiles are used as the base state in a horizontally homogeneous control simulation.

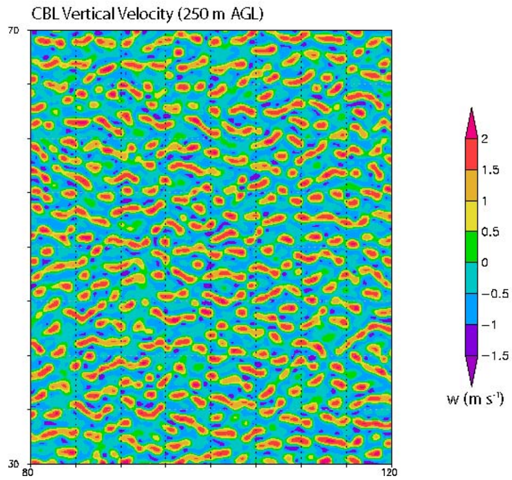

FIG. 3. Horizontal cross section of vertical velocity at 250 m AGL in the CBL simulation at 3600 s over a 40 km x 40 km subset of the domain.

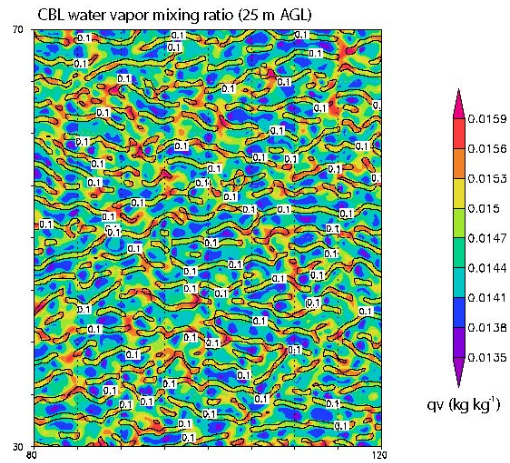

FIG. 4. Horizontal cross section of water vapor mixing ratio (shaded) at 25 m AGL over a 40 km x 40 km subset of the domain at 3600 s. The 0.1 m s^{-1} vertical velocity contour is plotted to indicate updraft location.

as much as 5 K within the anvil shadows of observed storms. In simulations including anvil shading, Frame et al. (2009) found that radiative cooling in the anvil shadow was enough to reverse the surface sensible heat flux such that the ground cools the boundary layer from below. As such, we hypothesize that boundary layer convection may be suppressed by cloud shading. This theorized decrease in convection, if supported by our simulations, is likely to lead to a decrease in the horizontal variability of storm-relevant parameters within the inflow region, provided that the anvil and solar angle are oriented such that the inflow region is shaded.

The ongoing research presented herein endeavors to clarify the interaction between supercell thunderstorms and the CBL. Section 2 presents the methodology used to simultaneously simulate a CBL and supercell thunderstorm. In section 3, results are presented pertaining to the characteristics of a CBL, the response of a supercell to the CBL, and the modification of the CBL by the storm within our numerical simulations. Preliminary conclusions and avenues of future research are discussed in section 4.

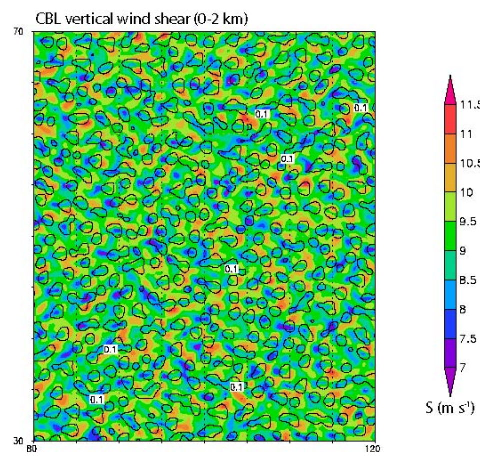

FIG. 5. Horizontal cross section of 0-2 km wind shear (shaded) at 3600 s over a 40 km x 40 km subset of the CBL simulation domain. The 0.1 m s^{-1} vertical velocity contour at 1 km AGL is plotted to indicate updraft location.

2. Methods

Two high-resolution numerical simulations were conducted in order to compare a supercell initiated in a horizontally-homogeneous environment with one initiated in a CBL composed of quasi-linear, HCR-like circulations. Despite significant research interest in the initiation of deep convection by boundary layer processes, this experiment is focused on the evolution of mature storms within a CBL. Because the homogeneous control experiment has no means of initiating convection, the CBL experiment also purposely is limited in its ability to independently initiate deep convection.

2.1 Model configuration

Both experiments are run using CM1, Release 14 (Bryan and Fritsch 2002; Bryan 2002) with the addition of radiation and land surface parameterizations. The simulations are run on a domain that is 200 km in the east-west direction, 150 km in the north-south direction and 18 km in the vertical direction. The horizontal grid spacing is constant at 200 m, whereas the vertical grid spacing is stretched from 50 m below 3 km to 500 m above 9.5 km. The corresponding large time step used to maintain the CFL criterion is 0.75 s with an acoustic time step of 0.125 s. Periodic boundary conditions are used on the lateral boundaries while a rigid lid is in place at the top of the domain with a Rayleigh damping sponge layer applied above 14 km. The ice phase microphysical parameterization developed by Lin et al. (1983) is used. A radiation scheme that includes absorption, emission, and scattering of both long and short wave radiation is added to CM1 for the CBL simulation with radiative forcing updated every 900 s. Furthermore, a two-layer soil model (Noilhan and Planton 1989) is implemented in the CBL simulation.

Because the base state does not include a large-scale tem-

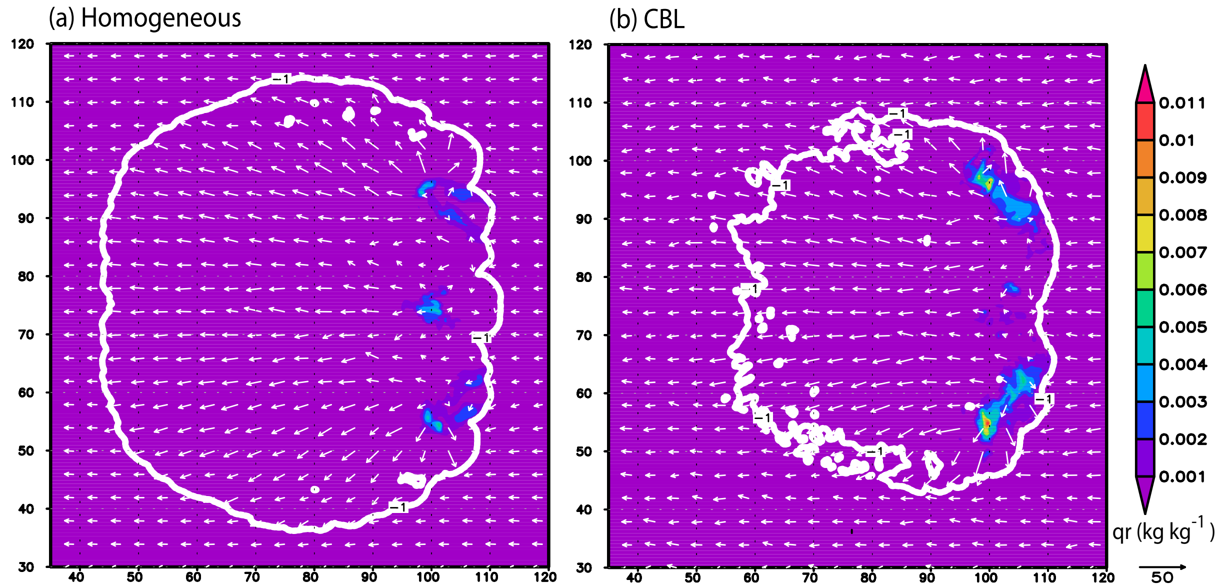

FIG. 6. Horizontal cross sections of wind, qr (shaded), and -1 K potential temperature perturbation (contour) at 25 m AGL in the (a) homogeneous and (b) CBL simulations at 9000 s.

perature gradient and the Coriolis force is neglected, there is no restoration of thermal wind balance by the model. Therefore, vertical momentum fluxes quickly mix out shear in the CBL simulation. In order to simulate supercells, we desire to maintain low-level vertical wind shear. Thus, a variation of the approach put forth by Robe and Emmanuel (2001) is used to maintain the wind shear. Similar to the Rayleigh damping technique used at upper levels in the domain, the horizontal winds at each grid point are relaxed towards the initial state by adding a tendency to every grid point and every timestep. This tendency is constant for each horizontal level, and thus leaves kinematic quantities such as vertical vorticity and divergence undisturbed. The tendency is re-calculated every timestep to maintain the average wind shear in low levels.

2.2 *Initial state and model initialization*

The CBL simulation is initialized using a unidirectional wind profile characterized by 35 m s^{-1} of 0-6 km shear and a thermodynamic profile similar to that used by Bluestein and Weisman (2000) and Knopfmeier et al. (2008) that contains a small capping inversion to limit initial convection to the boundary layer (Fig. 1). The model is initialized with a solar angle corresponding to a location of 38.7°N, 98.4°W (Northern Oklahoma) at 10:00 CDT on 15 May. In order to develop boundary layer convection, random temperature perturbations with amplitude ≤0.5 K are inserted in the lower levels of the domain. The model is run for 1 h and then stopped when boundary layer convection has developed. Next, the vertical wind and thermodynamic profiles of the CBL simulation at 1 h are horizontally averaged (Fig. 2) and used as the base state for a horizontally-homogeneous simulation.

The CBL and homogeneous simulations have a similar model configuration except that the homogeneous simulation is run without radiation, soil parameterizations, or surface fluxes of temperature, moisture, and momentum. This is required because it was found that, despite the horizontally uniform base state, the addition of a warm bubble perturbation and subsequent storm development resulted in enough heterogeneity to trigger a convective boundary layer in an initially homogeneous simulation that included surface fluxes. Though CAPE does increase with time owing to surface sensible and latent heat fluxes in the CBL simulation, the use of the average thermodynamic profile after one hour for the homogeneous simulation base state partially mitigates this discrepancy.

After one hour of CBL evolution, the CBL simulation is restarted, including a warm bubble with a maximum perturbation of 3 K that has a horizontal radius of 10 km and vertical radius of 1.5 km. The bubble center is in the middle of the horizontal domain and 1.5 km above the lower model surface. This is identical to the initiation used in the homogeneous simulation that is without a CBL. Both simulations are continued for two hours during which deep convection evolves.

3. Results

3.1 *Characteristics of a simulated convective boundary layer*

The simulation initialized with a horizontally-heterogeneous initial state develops a CBL with characteristics similar to those observed in the atmosphere. Random potential temperature perturbations grow with time as the boundary layer is heated from below. Small scale updrafts or thermals develop as a consequence of the uneven horizontal temperature distribution and convectively unstable boundary layer. By 3600 s, the low-level vertical velocity field has evolved into a quasi-linear pattern similar to HCRs (Fig. 3). The long axes of these features are arranged parallel to the low-level mean wind and shear vector. Vertical velocity maxima of up to 2 m s^{-1} are separated by approximately 2 km. At higher levels in the boundary layer (not shown), the thermals become less linear in nature (compare Figs. 3-5).

CBL water vapor mixing ratio (Fig. 4) has increased from the initial value of 13 g kg^{-1} across the entire domain owing to parameterized evaporation of soil moisture. Air moistened by the surface moisture flux has collected under updraft regions, increasing qv there to nearly 16 g kg^{-1}, whereas qv in downdraft regions is at a minimum (presumably due to advection of drier air from aloft).

Horizontal perturbations to the wind field associated with CBL circulations have led to horizontal heterogeneity in low-level wind shear as well. The domain average 0-2 km wind shear is 9.3 m s^{-1}. Figure 5 shows deviations from this average of up to +/- 2 m s^{-1}. Unlike heterogeneities in temperature and moisture, maxima in shear are not co-located with vertical velocity maxima in accord with Markowski and Richardson (2007).

3.2 *Comparison of supercells simulated in horizontally-homogeneous and CBL environments*

In both simulations, the warm bubble perturbation evolves into splitting supercell thunderstorms. Both the right and left-moving storms are of comparable intensity, as expected given the unidirectional wind profile. By 9000 s, an extensive cold pool has developed from the outflow of the storms in each simulation (Fig. 6). The cold pool in the homogeneous simulation has propagated over 10 km farther west than in the CBL simulation. Furthermore, the upshear (western) boundary of the cold pool is more diffuse in the CBL simulation. The rainwater mixing ratio reaches greater values near the surface in the CBL simulation and has a larger areal extent than in the homogeneous simulation. This difference in qr also was observed by Knopfmeier et al. (2008).

Time series of maximum vertical velocity (Fig. 7), maximum vertical vorticity at the surface (Fig. 8a) and maximum vertical vorticity at 4 km AGL (Fig. 8b) suggest that the storms have updrafts and rotation of similar intensity. Though both simulations have similar average values of maximum surface vertical vorticity, the CBL simulation has a significantly larger overall maximum around 9600 s. This maximum corresponds to a transient low-level vortex located on the tip of a reflectivity feature in the model similar to a hook echo (not shown). At 4 km AGL the simulations have similar averages in maximum vertical vorticity, but again the CBL simulation has a larger overall maximum.

Horizontal cross sections of vertical velocity and vertical vorticity at 9000 s (Fig. 9) reveal more subtle differences between the simulations. At low-levels (Figs. 9a,b) both storms have maxima in vertical velocity along the gust front. Though slightly stronger, the updraft along the CBL gust front has a more ragged appearance than in the homogeneous simulation, particularly farther to the south. Local vorticity maxima exist along notches in the CBL storm gust front, but these features are largely absent from the homogeneous storm. The cold pools

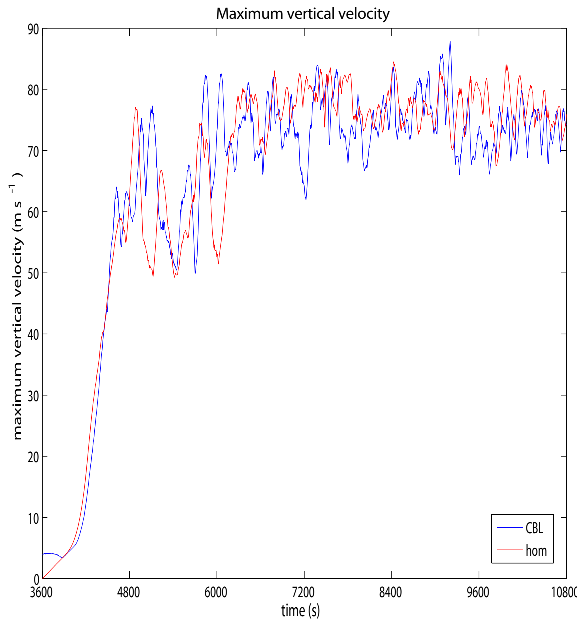

FIG. 7. Time series of maximum vertical velocity in the CBL (blue) and homogeneous (red) simulations.

of the two storms are characterized by similar horizontal variability in vertical velocity, but in the CBL simulation horizontal variability also exists in that storms inflow region.

At 4 km AGL, the simulations have similar vertical velocity and vertical vorticity magnitudes but differences in structure (Figs. 9c,d). Again, the vertical velocity field is considerably smoother in the homogeneous simulation, whereas the CBL simulation has large horizontal heterogeneity. Vertical vorticity, though of similar magnitude to the CBL simulation, is generally confined to regions near the main updraft and downdrafts in the homogeneous simulation. As in the vertical velocity field, the vertical vorticity field has a significant amount of horizontal variance in the CBL storm. There are numerous vorticity maxima greater than 0.02 s^{-1} at 4 km AGL, above the surface outflow and inflow regions of the CBL storm (SW and SE of the precipitation core), whereas these features are not present in the homogeneous simulation.

3.3 *Effects of supercells on the CBL*

In addition to the effects of a CBL on storm evolution, the presence of a supercell alters the convective boundary layer. As one might expect, storm outflow appears to disrupt boundary layer convection. Figure 10 shows a clearly defined gust front on the edges of the cold pool. Within the cold pool, perturbation vertical velocities are significantly weakened relative to the ambient environment. Boundary layer thermals also are suppressed underneath the anvil of the storms. The anvil (not shown) spreads downshear of the storms casting a shadow east of the deep convection. Through a reduction of solar shortwave radiation reaching the surface, the soil temperature cools up to 6 K in this region. As in the cold pool, thermals with vertical velocities greater than 2 m s^{-1} are greatly diminished in this region.

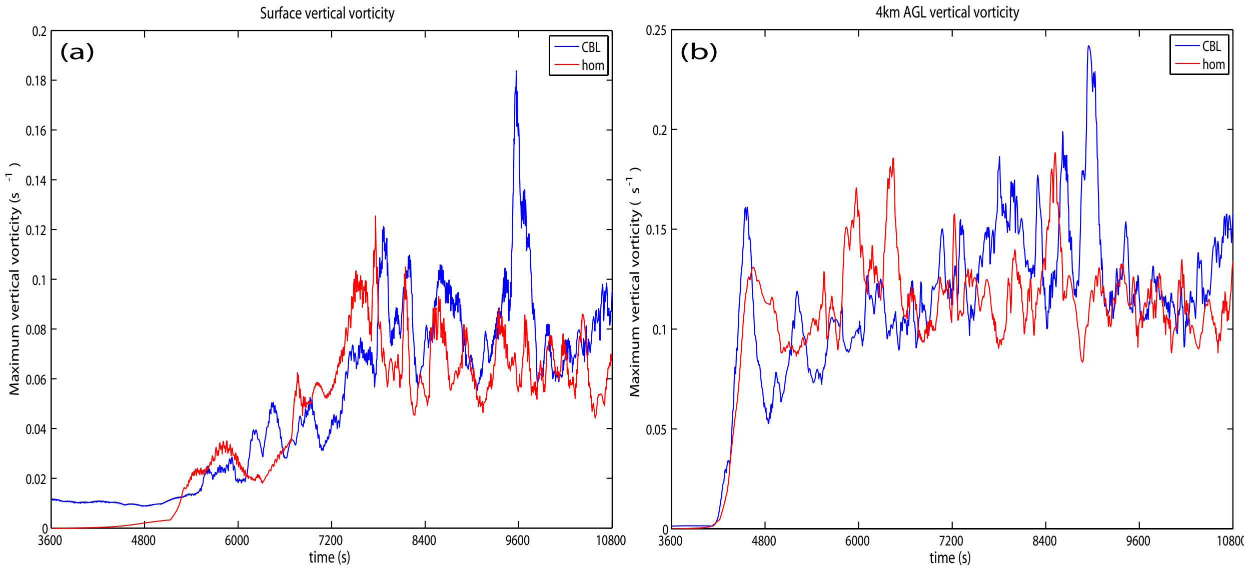

FIG. 8. Time series of maximum (a) surface and (b) 4km AGL vertical vorticity in the CBL (blue) and homogeneous (red) simulations.

4. Conclusions and future work

Though time series suggest little difference in maximum vertical velocity and vertical vorticity (common measures of bulk storm strength), fine scale differences exist between supercells simulated in a horizontally-homogeneous environment with no surface fluxes and those in an environment with a realistic CBL. These preliminary results suggest that the structure of storm features may be sensitive to CBL features. Unresolved questions exist as to why storms in CBL simulations have more rainwater, why the cold pool extends farther in a homogeneous case, and how storms alter a CBL. In the future, different thermodynamic and wind profiles may be chosen to more carefully control the structure of the boundary layer convection. Furthermore, the effects of the orientation of two dimensional CBL features relative to storm motion may be explored. The effects of anvil shading on boundary layer convection in the storm environment may also prove important, particularly when the storm inflow is shaded. Therefore, a more accurate representation of cloud shading using the tilted independent pixel approximation will be included in future simulations.

Acknowledgments. This research was funded by NSF grant AGS-0644533. Travel was supported by the NCAR Mesocale and Microscale Meteorology Division. Computing support and resources were provided by NCAR CISL. Special thanks go to Jim Marquis, Ryan Hastings, and Andrew Oberthaler for helpful input and enlightening discussions as well as Rich Rotunno for suggestions regarding the maintence of low-level shear in simulations with a CBL.

REFERENCES

Bluestein, H. B., and M. L. Weisman, 2000: The interaction of numerically simulated supercells initiated along lines. *Mon. Wea. Rev.*, **128**, 3128–3149.

Bryan, G. H., 2002: An investigation of the convective region of numerically simulated squall lines. Ph.D. thesis, The Pennsylvania State University, 181 pp.

——, and J. M. Fritcsh, 2002: A benchmark simulation for moist nonhydrostatic numerical models. *Mon. Wea. Rev.*, **130**, 2917–2928.

Carpenter, R. L., K. K. Droegemeier, and A. M. Blyth, 1998: Entrainment and detrainment in numerically simulated cumulus congestus clouds. Part I: General results. *J. Atmos. Sci.*, **55**, 3417–3432.

Etling, D., and R. A. Brown, 1993: Roll vortices in the planetary boundary layer: A review. *Bound. Layer Meteor.*, **65**, 215–248.

Frame, J. W., J. L. Petters, P. M. Markowski, and J. Y. Harrington, 2009: An application of the tilted independent pixel approximation to cumulonimbus environments. *Atmos. Res.*, **91**, 127–136.

Knopfmeier, K. H., P. M. Markowski, and Y. P. Richardson, 2008: Numerical simulations of supercells in convective boundary layers, Preprints, 24th Conf. on Severe Local Storms, Savannah, GA, Amer. Meteor. Soc.

Lin, Y.L., R. D. Farley, and H. D. Orville, 1983: Bulk parameterization of the snow field in a cloud model. *J. Climate Appl. Meteor.*, **22**, 1065–1092.

Markowski, P. M., E. N. Rasmussen, J. M. Straka, and D. C. Dowell, 1998: Observations of low-level baroclinity generated by anvil shadows. *Mon. Wea. Rev.*, **126**, 2942–2958.

—— and Y. P. Richardson, 2007: Observations of vertical wind shear heterogeneity in convective boundary layers. *Mon. Wea. Rev.*, **135**, 843–861.

—— and ——, 2009: Tornadogenesis: Our current understanding, forecasting considerations, and questions to guide future research. *Atmos. Res.*, **93**, 3–10.

Noilhan, J., and S. Planton, 1989: A simple parameterization of land surface processes for meteorological models. *Mon. Wea. Rev.*, **117**, 536–549.

Peckham, S. E., R. B. Wilhelmson, L. J. Wicker, and C. L. Ziegler, 2004: Numerical simulation of the interaction between the dryline and horizontal convective rolls. *Mon. Wea. Rev.*, **132**, 1792–1812.

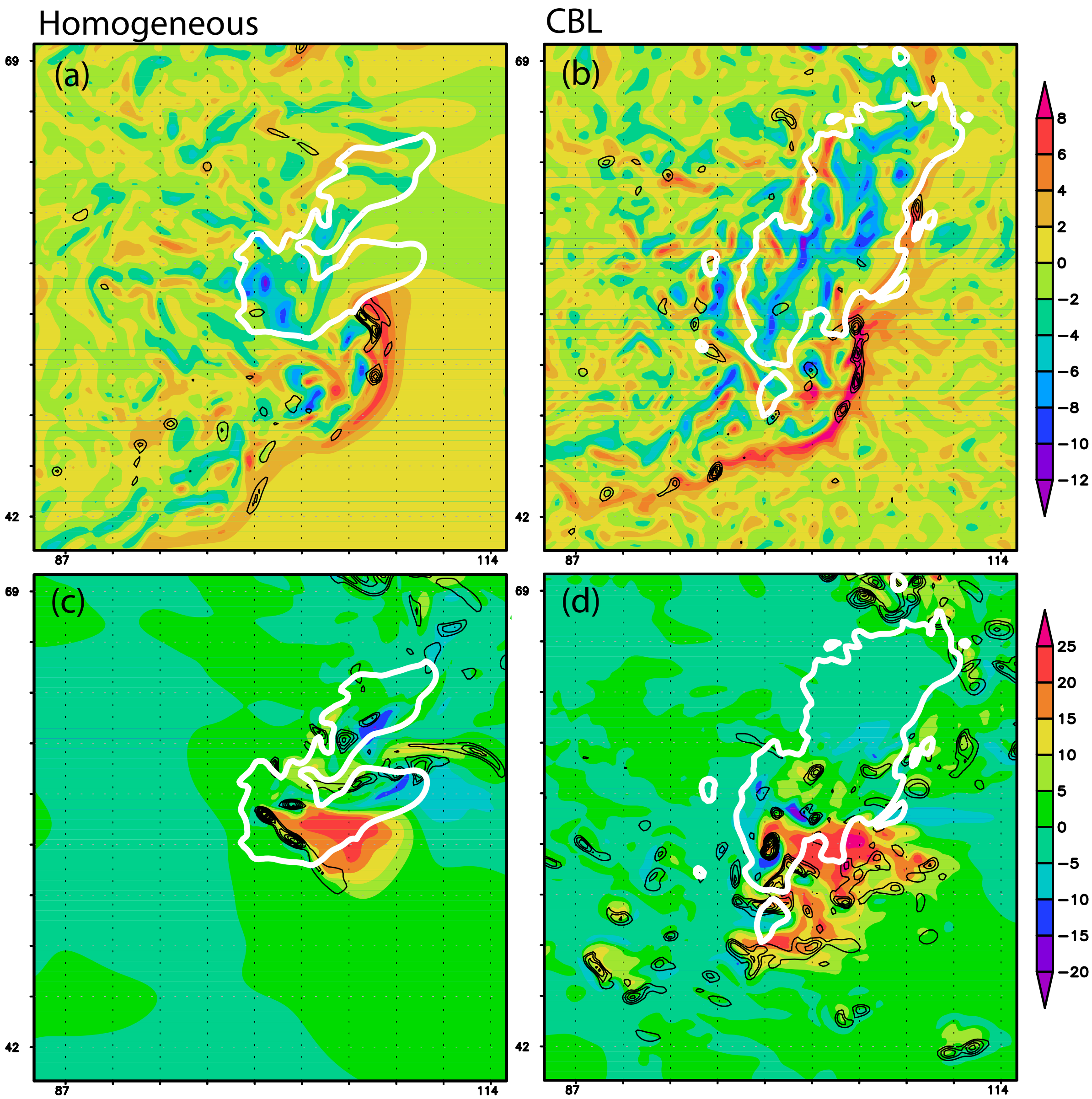

FIG. 9. Horizontal cross sections of w (m s^{-1}, shaded) at 500 m AGL, positive vertical vorticity (contoured in black at 0.01 s^{-1} intervals) at 25 m AGL, and the 0.001 kg kg^{-1} qr isopleth (white contour) for the (a) homogeneous and (b) CBL simulations at 9000 s in the right-moving storm. (c) and (d) are the same, but with w and vertical vorticity at 4 km AGL.

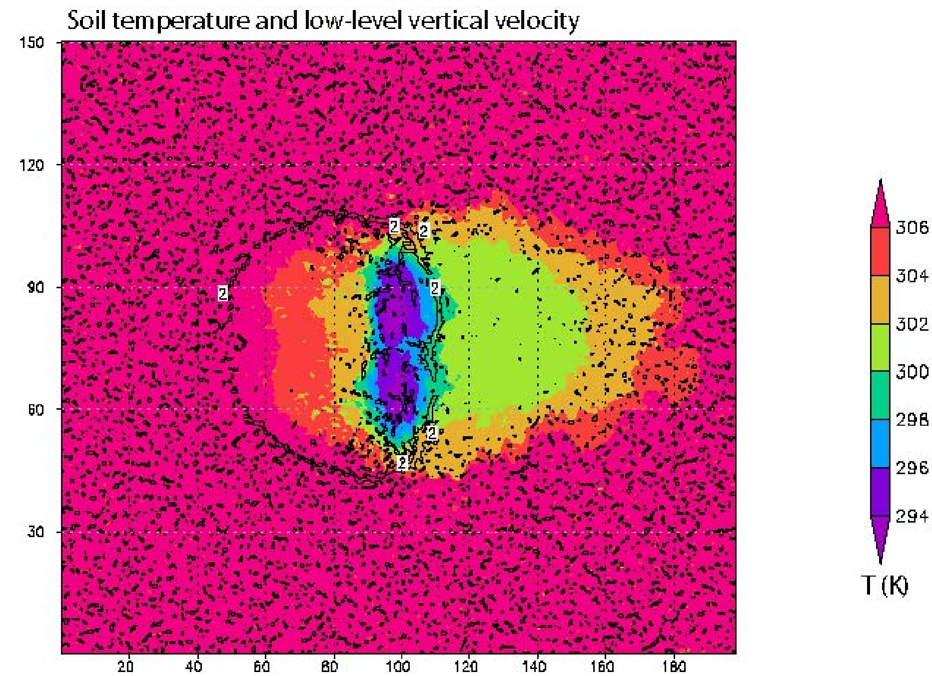

FIG. 10: Soil temperature (shaded) and vertical velocity at 500 m AGL (2 m s^{-1} contour shown) at 9000 s.

Richardson, Y. P., 1999: The influence of horizontal variations in vertical shear and low-level moisture on numerically simulated convective storms. Ph.D. dissertation, School of Meteorology, University of Oklahoma, 236 pp.

———, K. K. Droegemeier, and R. P. Davies-Jones, 2007: The influence of horizontal environmental variability on numerically simulated convective storms, Part I: Variations in Vertical Shear. *Mon. Wea. Rev.*, **135**, 3429–3455.

Robe, F. R. and K. A. Emanuel, 2001: The effect of vertical wind shear on radiative-convective equilibrium states. *J. Atmos. Sci.*, **58**, 1427–1445.

Weckwerth, T. M., J. W. Wilson, and R. M. Wakimoto, 1996: Thermodynamic variability within the convective boundary layer due to horizontal convective rolls. *Mon. Wea. Rev.*, **124**, 769–784.

———, T. W. Horst, and J. W. Wilson, 1999: An observational study of the evolution of horizontal convective rolls. *Mon. Wea. Rev.*, **127**, 2160–2179.

Weisman, M. L., and J. B. Klemp, 1982: The dependence of numerically simulated convective storms on vertical wind shear and buoyancy. *Mon. Wea. Rev.*, **110**, 504–520.